Time Series Modelling of Paleoclimate Data
– *Supporting Information*

J. E. H. Davidson, University of Exeter
D. B. Stephenson, University of Exeter
A. A. Turasie, University of Witwatersrand

Introduction

This supplement contains tables and charts associated with the results in Davidson et al (2015), and needs to be read in conjunction with that article.

1 The Data

The EPICA data sets consist of paired magnitudes and imputed dates, which are irregularly spaced. Values are imputed to 1 kyr intervals by linear interpolation; in other words, by joining the (recorded value, recorded date) pairs by straight lines and reading off the values of this continuous record at the chosen time intervals. Temperature is recorded in degrees Celsius, CO_2 and CH_4 concentrations are expressed in parts per 10^4. The ice volume series has also been interpolated linearly, but this effects only a few of the early observations at 2kyr intervals. The proxy is the percentage of the δ^{18}O isotope of oxygen in benthic core samples. Figure 1 shows the resulting series, before logarithmic transformation, and Table 1 shows summary statistics for these series. Figure 2 shows histograms and kernel densities for the raw series of Figure 1 of this supplement (top row) and the logarithmically transformed series in Figure 1 of the paper (second row).

Figure 3 shows the autocorrelations of the logarithmic series. The partial sums of these sequences are plotted in Figure 4, and the partial sums of the absolute values in Figure 5. The contrast between these sequences, the absolute sums diverging while the signed sums diminish, may be indicative of the failure of the HML test in Appendix A of the paper to yield results matching the other tests of the 'I(0)' hypothesis. Another view of these series properties is provided by Figure 6 which shows the smoothed periodograms of the series plotted on the interval $[0, \pi]$. While these estimated spectral densities are large close to the origin, there is clearly no evidence of divergence at the origin.

	Temp.	CO_2	CH_4	Ice
Maximum	3.76	2.94	7.89	5.08
Minimum	−10.25	1.72	3.46	3.10
Mean	−5.29	2.23	4.95	4.17
Std. Dev.	2.90	0.25	0.81	0.44
Skewness	0.71	0.37	0.55	−0.23
Kurtosis	2.90	2.32	2.73	2.34

Table 1: Summary statistics

	Temp.	CO_2	CH_4	Ice
s_{AR}	0.0893	0.0357	0.0638	0.0612
Sample initial value X_0	1.998	0.642	1.442	1.543
$\overline{b}$ = sample maximum	2.984	1.082	2.065	1.625
$\underline{b}$ = sample minimum	1.748	0.546	1.242	1.131
$\widehat{\overline{c}}$	0.417	0.613	0.345	0.047
$\widehat{\underline{c}}$	−0.106	−0.135	−0.111	−0.238

Table 2: Simulation parameters for unit root tests subject to barriers

2 Tests for a Bounded Random Walk

Cavaliere and Xu (2014) derive the limit distribution of the ADF statistic under the hypothesis of a bounded random walk process, and show that this depends on a regulated Brownian motion $B_{\underline{c}}^{\overline{c}}$ where $\overline{c}$ and $\underline{c}$ are nuisance parameters. They show that $\overline{c}$ and $\underline{c}$ can be consistently estimated by the formulae

$$\begin{aligned} \widehat{\overline{c}} &= T^{-1/2}(\overline{b} - X_0)/s_{AR} \\ \widehat{\underline{c}} &= T^{-1/2}(\underline{b} - X_0)/s_{AR} \end{aligned}$$

where T is sample size, $\overline{b}$ and $\underline{b}$ are the actual bounds observed, X_0 is the initial value of the sequence and s_{AR} denotes the autoregressive estimator of the long-run variance of the differences ΔX_t, defined as $s^2 = \sum_{j=-\infty}^{\infty} \mathrm{Cov}(\Delta X_t, \Delta X_{t-j})$. In a process with autoregressive representation $b(L)\Delta X_t = \varepsilon_t$ under the null hypothesis, where ε_t is uncorrelated with variance σ^2, it can be shown that $s^2 = \sigma^2/b(1)^2$, and s_{AR}^2 estimates this quantity via the ADF fitted autoregression. The test is implemented by simulating the augmented Dickey-Fuller statistic with artificial bounded random walks, with bounds $\widehat{\overline{c}}$ and $\widehat{\underline{c}}$ and independent Gaussian shocks ε_t^* having variance $1/T$. In our implementation, the bounds are imposed in the simulations by the data generating equation

$$X_t^* = \widehat{\overline{c}} + ((X_{t-1}^* + \varepsilon_t^* - \widehat{\underline{c}})^+ + \widehat{\underline{c}} - \widehat{\overline{c}})^-$$

where $(.)^+$ and $(.)^-$ denote respectively the positive and negative parts of their arguments. The statistics used in the construction of the test tabulations in Table 2 of the paper, estimated by 5000 Monte Carlo replications of the ADF statistics, are shown in Table 2. The artificial samples were of size $T = 798$ to match the length of the observed series, and the number of lagged terms in the statistics match those reported in Table 8 of the paper.

3 VECM Model Results

The model, represented by equation (3) of the paper with the addition of intercepts, is estimated by Gaussian maximum likelihood. The estimates of the matrices $\boldsymbol{E}$ and $\boldsymbol{\Pi}$ are given as Tables 5 and 7 of the paper. The estimates of the coefficients of $\boldsymbol{D}(L)$ and $\boldsymbol{C}(L)$ and the GARCH coefficients $\sqrt{\boldsymbol{\omega}}$, $\boldsymbol{\delta}$ and $\boldsymbol{\beta}$ are in Table 3 of this supplement. The star decorations in these and subsequent tables denote statistical significance according to asymptotically valid criteria, at the 10% (*), 5% (**) and 1% (***) levels respectively. The reported standard errors are computed from the robust estimator of the covariance matrix having the form $\boldsymbol{V} = \boldsymbol{Q}^{-1}\boldsymbol{P}\boldsymbol{Q}^{-1}$ where $\boldsymbol{P}$ denotes the covariance matrix of the scores, and $\boldsymbol{Q}$ the Hessian matrix of the criterion function. The information matrix equality $\boldsymbol{P} = -\boldsymbol{Q}$ is therefore not invoked, as befits the case when Gaussianity of the disturbances is not assumed. This table shows that there are important

	ΔTemp	ΔCO_2	ΔCH_4	ΔIce
Intercept	1.051 (0.664)	0.182 (0.202)	0.886 (0.0.577)	-0.473^{*} (0.260)
AR1(ΔTemp)	0.0037 (0.052)	0.001 (0.014)	0.067^{*} (0.038)	-0.013 (0.014)
AR1(ΔCO_2)	0.897^{***} (0.140)	0.358^{***} (0.054)	0.191 (0.111)	-0.068 (0.045)
AR1(ΔCH_4)	-0.024 (0.041)	0.026^{*} (0.013)	0.014 (0.044)	0.001 (0.014)
AR1(ΔIce)	-0.103 (0.103)	-0.071^{**} (0.030)	0.124 (0.087)	-0.037 (0.042)
AR2(ΔTemp)	-0.104^{**} (0.044)	-0.0047 (0,111)	0.073^{**} (0.031)	0.013 (0.013)
AR2(ΔCO_2)	0.075 (0.121)	-0.185^{***} (0.045)	0.279^{***} (0.106)	0.025 (0.046)
AR2(ΔCH_4)	-0.048 (0.031)	-0.0003 (0.010)	0.036 (0.032)	0.010 (0.011)
AR2(ΔIce)	-0.074 (0.096)	-0.051 (0.036)	0.025 (0.086)	0.051 (0.047)
ΔEccentricity	-4.795 (27.35)	-11.54 (9.39)	1.090 (25.23)	-20.03 (12.43)
ΔEccentricity(-1)	25.37 (28.18)	17.56^{*} (10.06)	-4.83 (25.34)	14.69 (12.66)
ΔObliquity	-3.219^{***} (1.233)	-0.373 (0.375)	-1.584 (1.062)	1.192^{**} (0.469)
ΔObliquity(-1)	3.246^{**} (1.239)	0.389 (0.375)	1.646 (1.062)	-1.21^{**} (0.469)
ΔPrecession	-15.46^{**} (7.20)	-6.07^{**} (2.38)	6.347 (6.618)	3.054 (2.417)
ΔPrecession(-1)	14.88^{**} (7.287)	6.18^{**} (2.39)	-7.606 (6.178)	-2.729 (2.421)
GARCH $\sqrt{\omega}$	0.028 (0.004)	0.013 (0.001)	0.042 (0.004)	0.019 (0.002)
GARCH δ	0.993^{***} (0.035)	0.824^{***} (0.092)	0.508^{**} (0.208)	0.663^{***} (0.1775)
GARCH β	0.685^{***} (0.065)	0.345^{***} (0.091)	0.046 (0.191)	0.480^{**} (0.240)

Table 3: Estimates of $\boldsymbol{C}(L)$ and $\boldsymbol{D}(L)$ elements and GARCH parameters (robust standard errors in parentheses) .

contributions to each equation from the current and lagged changes in the orbital variables although these effects appear to be largely off-setting; in other words, it is the second differences of the cycles that appear to matter most.

Figures 7 and 8 show the residuals from the mean equations with two-standard error bands, respectively before, and after, normalization by $1/\sqrt{\boldsymbol{h}_t}$. While symmetrically distributed, the normalized residuals appear distinctly heavy-tailed in Figure 8. Figure 9 shows the series defined by the deviations from equation 4 of the paper, expressed in centred (mean deviation) form in view of the the inclusion of unrestricted intercepts in the dynamic relations. These curves are dominated by the orbital cycles but not by the glacial cycles, showing that the steady-state relation between $\boldsymbol{x}_t$ and $\boldsymbol{d}_t$ does succeed broadly in tracking the ice ages, even though there are substantial higher frequency oscillations that need to be accounted for by the system dynamics.

Table 4 shows the optimized value of the log-likelihood and system diagnostics, specifically the Lagrange multiplier and conditional moment test statistics for system-wide autocorrelation, neglected ARCH effects, and nonlinearity. These alternative test principles are based in the first case on the scores of the log-likelihood function in the extended model, and in the second

Log-likelihood: 8392.92

System tests:	Lagrange multiplier	Conditional Moment
Autocorrelation (32):	39.51	14.23
Neglected ARCH (32):	41.39	37.23
Functional Form (16):	21.44	34.50***
Functional Form (32):	53.81***	66.73***

Table 4: System diagnostics. See text for details

	Temp	CO_2	CH_4	Ice
R^2 (levels)	0.915	0.962	0.882	0.960
Jarque-Bera Stat.	14.55***	108.3***	84.79***	52.82***
Box-Pierce (23)	23.62	21.82	17.55	13.12
McLeod-Li (25)	17.08	21.76	39.04	20.10

Table 5: Equation Diagnostics

case on the covariances of the residuals, or squared residuals, with the test variables. For the theory underlying these tests, see for example Davidson (2000) and references therein. In the present case the test variables are, respectively, the once and twice lagged residuals in the mean equations, the once and twice lagged squared residuals in the GARCH volatility equation and the squares, and squares and cubes, of the fitted model in the mean equations. The latter tests are generalizations of the RESET test (Ramsey 1969). The full set of test variables is included in each equation, resulting in the chi-squared degrees of freedom shown in parentheses.

The rejections in the functional form tests show the limitations of the linearization adopted, but it ought to be emphasized that with a large sample, where the tests have plenty of power, this type of result is not uncommon in econometric applications. Indeed, it must occur with probability one as the sample tends to infinity, unless the equations represent the actual data generation process in every respect. What matters most, from the point of view of making valid inferences, is that the equation residuals appear both uncorrelated and conditionally homoscedastic.

Table 5 contains equation-specific statistics. These include the R^2s (computed for levels, not differences) and univariate tests of autocorrelation (Box and Pierce 1970) and neglected ARCH (McLeod and Li, 1983) for the orders of lag shown in parentheses, These tests are designed for univariate models and their properties in a VAR context are not formally established, but they could indicate problems with particular equations, were these present. The Jarque-Bera (1980) test is for residual normality, which is rejected decisively. This finding indicates that our estimator is not true maximum likelihood but, as noted above, our inference procedures are designed to take account of this fact.

Table 6 shows the residual contemporaneous correlations, with star codes denoting rejections of the zero hypothesis in all but one case. Estimates of the correlations are mapped into the interval $[-1, 1]$ from the real line by the transformation $x/(1+|x|)$ where x is estimated unrestrictedly. The test outcomes reported are for the result of t-tests of the null hypotheses $x = 0$.

References

[1] Box, G. E. P., and D. A. Pierce (1970). The distribution of residual autocorrelations in autoregressive-integrated moving average time series models, *Journal of the American Statis-*

	Temp	CO_2	CH_4	Ice
Temp	1			
CO_2	0.455^{***}	1		
CH_4	-0.125^{***}	-0.129^{***}	1	
Ice	-0.170^{***}	-0.161^{***}	-0.018	1

Table 6: Residual correlation matrix

tical Association 5, 1509 26.

[2] Davidson, J. E. H., D. B. Stephenson and A. A. Turasie (2015) Time series modelling of paleoclimate data. *Environmetrics,* DOI: 10.1002/env.2373

[3] Jarque, C. M., and A. K. Bera (1980) Efficient tests for normality, heteroskedasticity and serial independence of regression residuals, *Economics Letters*, 6, 255-59.

[4] McLeod, A.I. and Li, W.K. (1983) Diagnostic checking ARMA time series models using squared-residual autocorrelations, *Journal of Time Series Analysis* 4, 269-273.

[5] Ramsey, J. B. (1969), J. B. (1969). Tests for specification errors in classical linear least-squares regression analysis, *Journal of the Royal Statistical Society, Series B*, 31, 350-71.

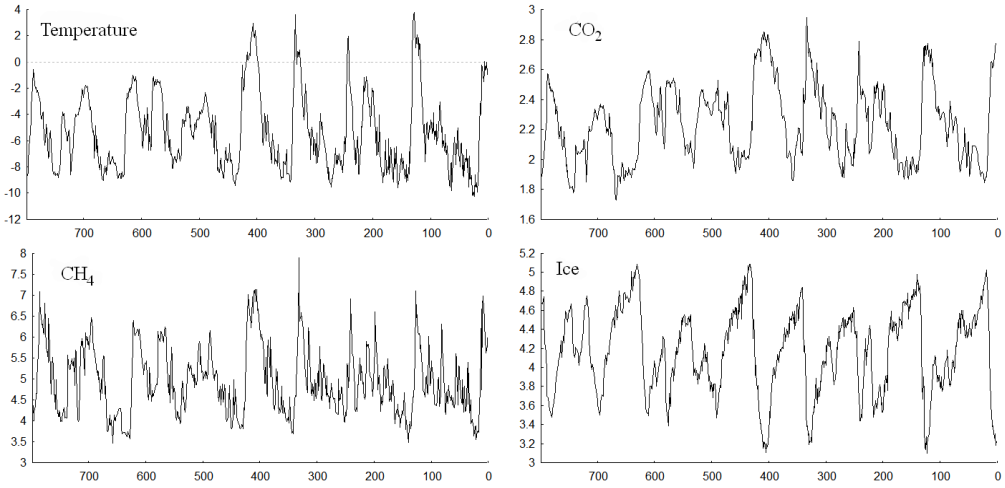

Figure 1: Recorded data, before transformation.

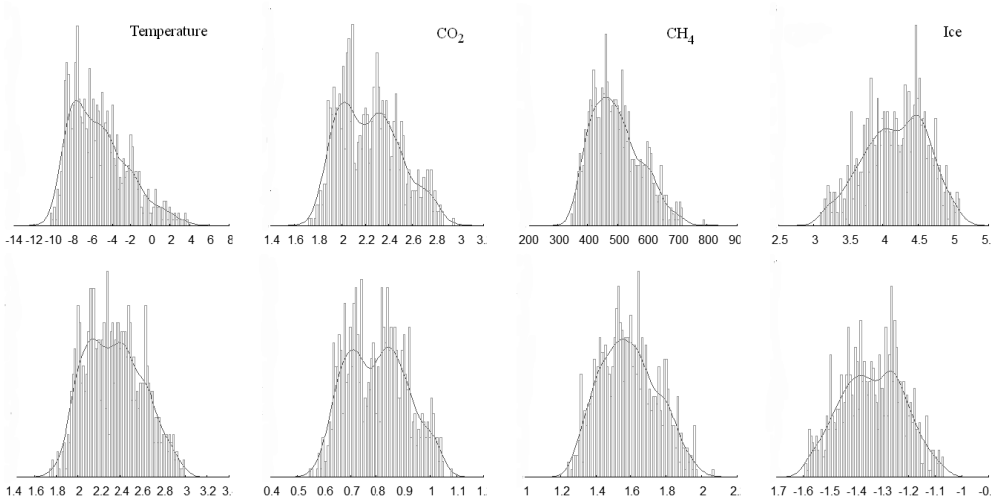

Figure 2: Series distributions

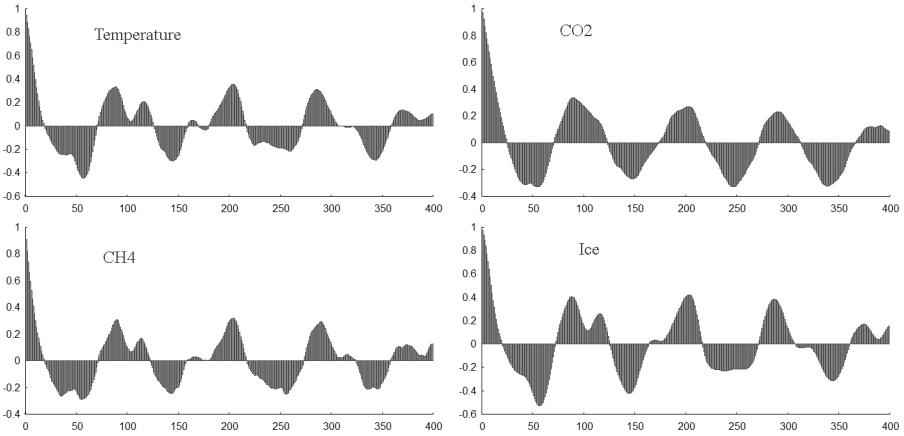

Figure 3: Autocorrelation functions of the logarithmic series

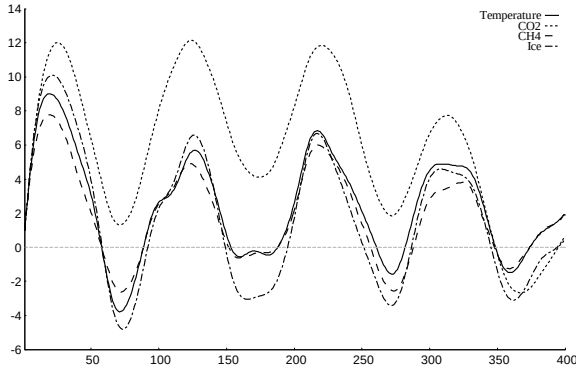

Figure 4: Cumulated autocorrelations of the logarithmic series.

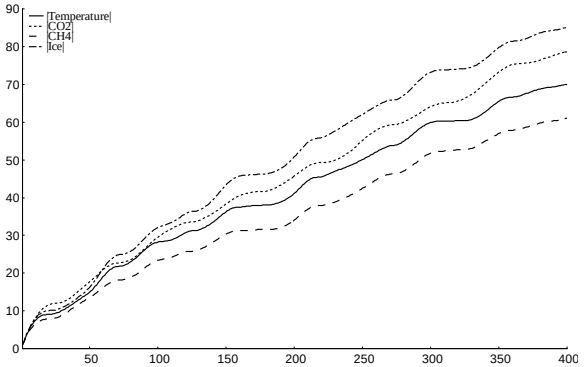

Figure 5: Cumulated absolute values of the autocorrelations.

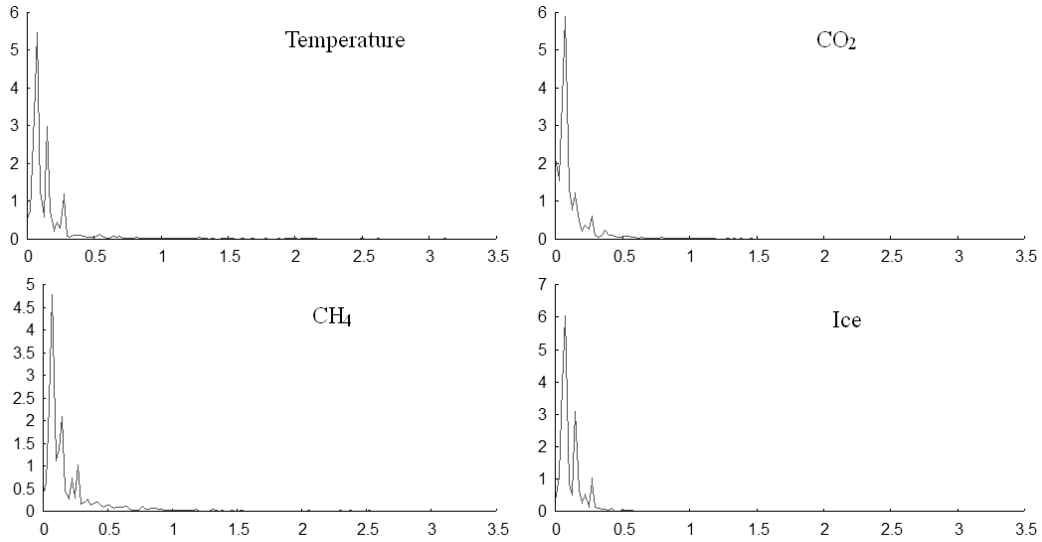

Figure 6: Smoothed periodograms

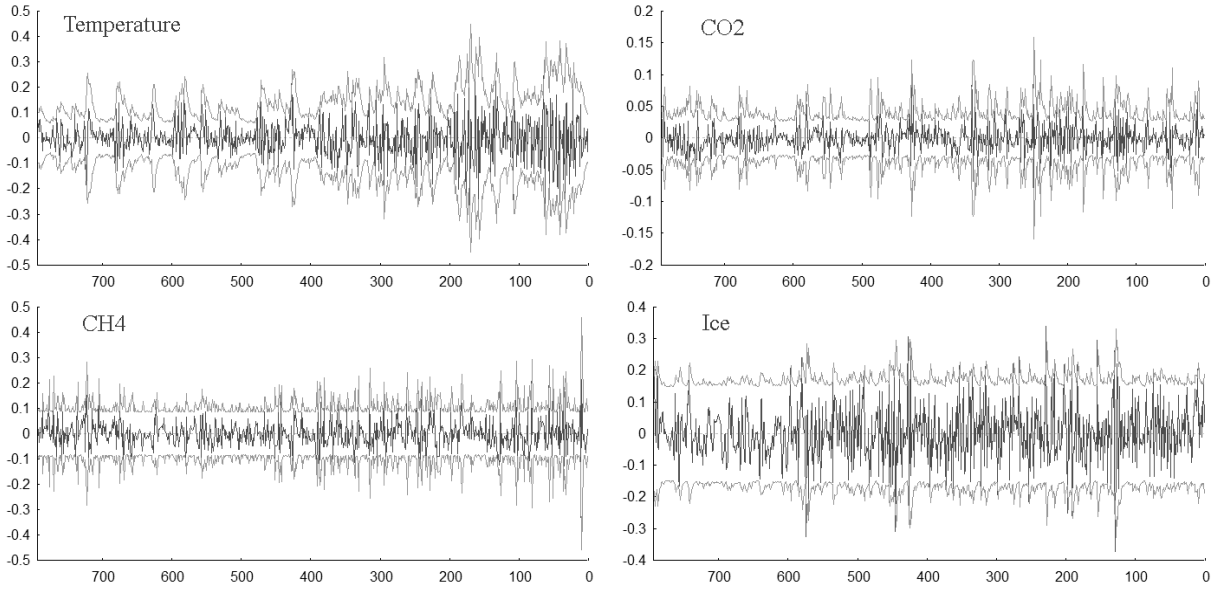

Figure 7: The unadjusted residuals, showing two-standard error bands estimated by the GARCH volatility model.

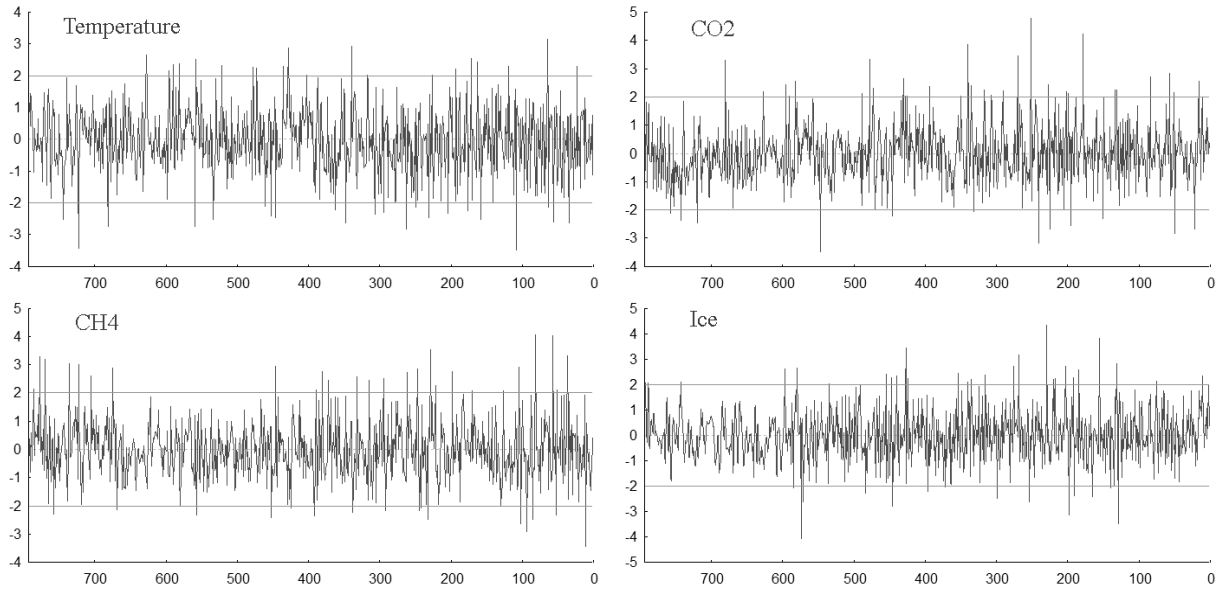

Figure 8: Residuals adjusted to unit variance

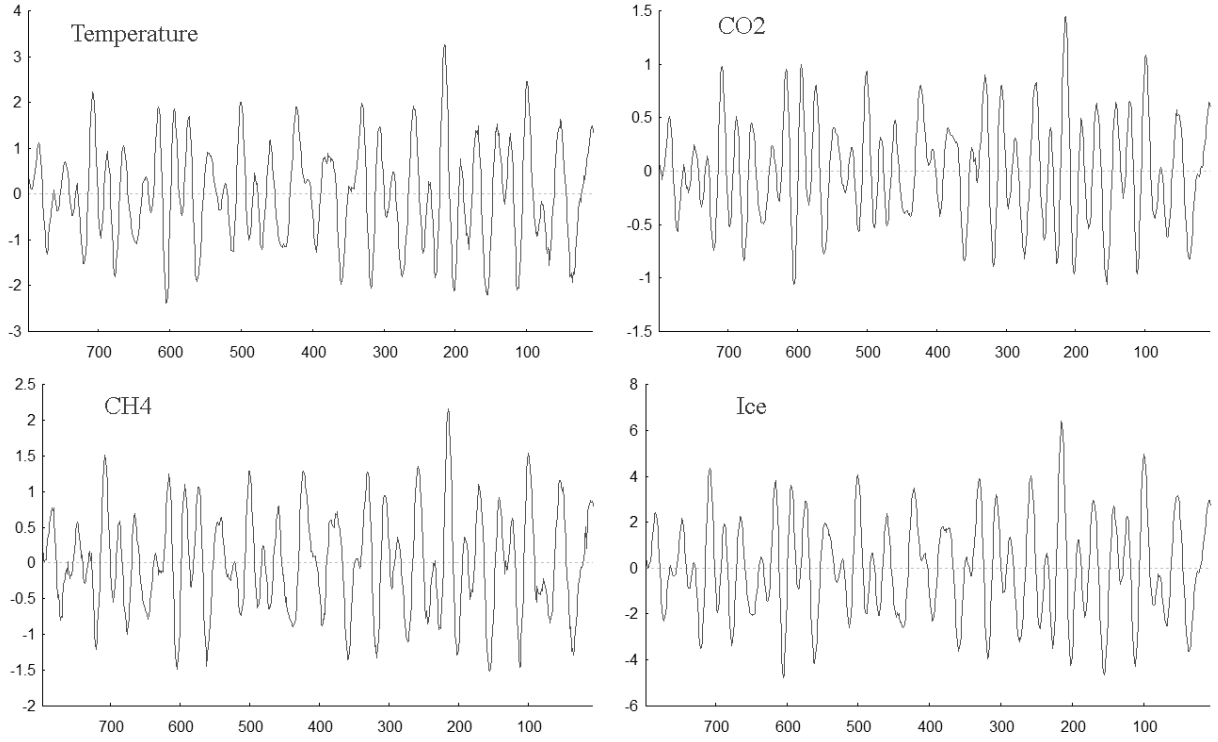

Figure 9: Deviations from steady-state relations.